CERN-ACC-2015-0022

christian.scheuerlein@cern.ch

Elastic anisotropy in multifilament Nb3Sn superconducting wires

C. Scheuerlein, B. Fedelich, P. Alknes, G. Arnau, R. Bjoerstad, B. Bordini
CERN, Geneva, Switzerland

Keywords: Nb3Sn, texture, elastic modulus, anisotropy, EBSD, tensile test

Abstract

The elastic anisotropy caused by the texture in the Nb3Sn filaments of PIT and RRP wires has been calculated by averaging the estimates of Voigt and Reuss, using published Nb3Sn single crystal elastic constants and the Nb3Sn grain orientation distribution determined in both wire types by Electron Backscatter Diffraction. At ambient temperature the calculated Nb3Sn E-moduli in axial direction in the PIT and the RRP wire are 130 GPa and 140 GPa, respectively. The calculated E-moduli are compared with tensile test results obtained for the corresponding wires and extracted filament bundles.

Presented at: ASC 2014, 10-15 August, Charlotte, USA

Geneva, Switzerland
February 2015

Elastic anisotropy in multifilament Nb_3Sn superconducting wires

C. Scheuerlein, B. Fedelich, P. Alknes, G. Arnau, R. Bjoerstad, B. Bordini

***Abstract*—The elastic anisotropy caused by the texture in the Nb_3Sn filaments of PIT and RRP wires has been calculated by averaging the estimates of Voigt and Reuss, using published Nb_3Sn single crystal elastic constants and the Nb_3Sn grain orientation distribution determined in both wire types by Electron Backscatter Diffraction. At ambient temperature the calculated Nb_3Sn E-moduli in axial direction in the PIT and the RRP wire are 130 GPa and 140 GPa, respectively. The calculated E-moduli are compared with tensile test results obtained for the corresponding wires and extracted filament bundles.**

***Index Terms*—Nb_3Sn, texture, elastic modulus, anisotropy, EBSD, tensile test**

I. INTRODUCTION

THE electro-magnetic properties of Nb_3Sn are strain sensitive. This has to be taken into account in the design of Nb_3Sn high field magnets like the 11 Tesla and large aperture quadrupole magnets being developed for the LHC luminosity upgrade [1], where the conductors are subject to high Lorentz forces. In order to derive the Nb_3Sn strain under a certain mechanical load, it is necessary to know the elastic constants of the different composite wire constituents, whose texture causes an elastic anisotropy.

Due to the heavy cold work during the wire drawing process the Cu matrix and the Nb pre-cursor are both strongly textured [2]. The brittle Nb_3Sn is formed when the conductor in its final size is submitted to a heat treatment [3,4]. The Nb_3Sn texture differs strongly in different conductor types. While in Bronze Route wires the Nb_3Sn grains have a nearly random orientation [5,6], we have observed a strong Nb_3Sn texture in Powder-in-Tube (PIT) [7] and in Restacked-Rod-Process (RRP) type superconductors. As revealed by non-destructive synchrotron X-ray diffraction [8], as well as by Electron Backscatter Diffraction (EBSD) [9], in the PIT wire the Nb_3Sn grains have a preferential <110> orientation, while in the RRP wire they have a strong <100> texture.

In this article we focus on the elastic anisotropy of the Nb_3Sn filaments in PIT and RRP type wires. Elastic moduli for polycrystalline Nb_3Sn have been calculated by averaging the estimates of Voigt and Reuss [10,11], using Nb_3Sn single crystal elastic constants and the Nb_3Sn grain orientation distribution in PIT and RRP-type conductors determined by EBSD [9]. Tensile tests of entire PIT and RRP wires and extracted filament bundles have been performed at room temperature (RT).

Nb_3Sn elastic constants are known to change strongly during cool down and a lattice softening is observed. The Nb_3Sn single crystal elastic constants used here for the calculations at RT and at 4.2 K are from [12] and [13], respectively.

In binary Nb_3Sn bulk with high Sn content of 24.5% or more, a cubic-to-tetragonal phase change occurs upon cooling at a temperature of roughly 30 K to 45 K [14,15,16]. For the calculations we have assumed that the Nb_3Sn lattice remains cubic at all temperatures, since the Sn content in the alloyed Nb_3Sn of multifilament wires is below 24.5% (apart from the coarse grain Nb_3Sn in PIT wires) [17].

II. EXPERIMENTAL

II.1 Nb_3Sn composite wires: The Nb_3Sn elastic anisotropy has been calculated using the grain orientation distribution measured in a PIT wire (billet number B215) produced by Shape Metal Innovation (now Bruker EAS) and in a RRP wire (billet number #7419) produced by Oxford Instruments Superconducting Technology [9]. Cross sections of the PIT wire after 650 °C-120 h heat treatment (HT) and of the RRP wire after 695 °C-17 h HT are shown in Figure 1.

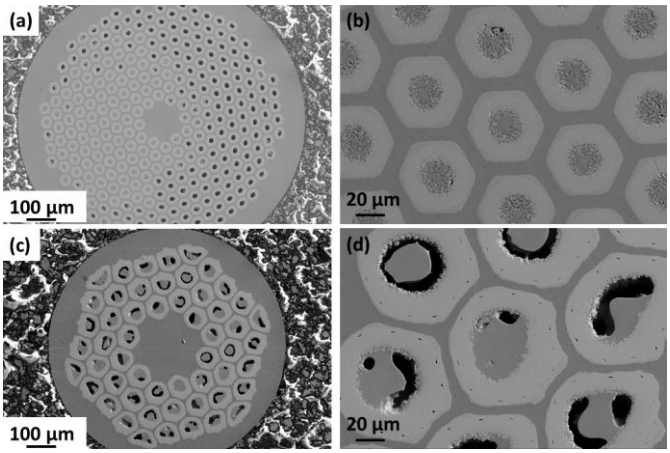

Figure 1: Metallographic cross sections of Nb_3Sn (a)-(b) PIT and (c)-(d) RRP wires.

In Figure 2 two PIT filament cross sections acquired after different heat treatments are compared. In the EBSD scans each crystal is given a certain color, according to its orientation. In Figure 2 (a) a PIT filament cross section is shown after a 620 °C-60 h HT. After this HT, part of the inner volume of Nb tube is transformed into Nb_6Sn_5 (see area in Fig.2 marked with ①). Between the outermost unreacted Nb

Manuscript received October 8, 2014.

P. Alknes, G. Arnau, B. Bordini, R. Bjoerstad and C. Scheuerlein are with CERN, CH-1211 Geneva 23, Switzerland, (corresponding author phone: ++41 (0)22 767 8829, e-mail: Christian.Scheuerlein@cern.ch).

B. Fedelich is with Federal Institute for Materials Research and Testing (BAM), 12205 Berlin, Germany.

precursor tube ② and the Nb_6Sn_5, a thin ring of very fine grained Nb_3Sn has been formed by solid state diffusion of Sn into Nb. In contrast, the ring of Nb_6Sn_5 has been formed from $NbSn_2$, which itself is formed when Sn starts to diffuse into the Nb tubes at about 520 °C [4].

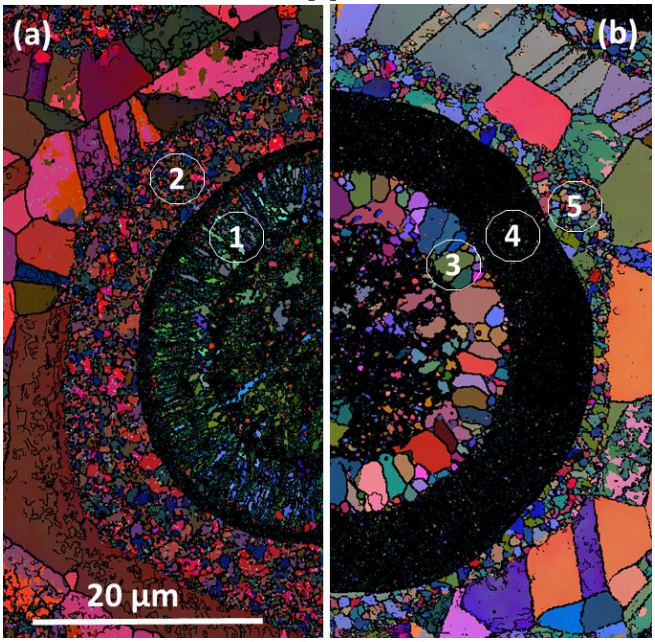

Figure 2: Euler angle maps of PIT filament (a) after 620 °C-60 h HT and (b) after 650 °C-120 h HT. The scale bar is valid for (a) and (b).

A cross section of a fully processed PIT filament is shown in Figure 2 (b). The filament consists of the filament core, a ring of coarse Nb_3Sn grains ③, which size is in the order of 1 µm, a ring of fine grained Nb_3Sn ④ with an average diameter of 0.16 µm and the unreacted Nb barrier ⑤. The fine Nb_3Sn grains are not resolved in the maps shown in Figure 2(b), and therefore appear as a black ring. High resolution Euler angle maps, in which the fine Nb_3Sn grains are resolved, are presented in [9]. The coarse Nb_3Sn grains are formed from Nb_6Sn_5.

The cross sectional areas of the different PIT and RRP wire and filament constituents, which have been determined by digital image analysis of the metallographic wire cross sections, are summarized in Table 1. The nominal diameters of these non-reacted PIT and RRP wires are 1.25 mm and 0.80 mm, respectively. About 10% of the RRP filament volume consists of porosity [18]. The porosity volume in the PIT wire is not well known.

Table 1: Characteristics of the fully processed wires for which the Nb_3Sn elastic anisotropy has been calculated.

	PIT B215 cross sections (mm^2)	RRP #7419 cross sections (mm^2)
Total wire	1.29 (1.29) [1]	0.537 (0.532) [1]
Non-Cu part	0.569	0.277
Unreacted Nb barrier	0.122 (21.4%)	0.0196 (7.1%)
Filament core	0.107 (18.8%)	0.0835 (30.1%)
Fine grain Nb_3Sn	0.238 (41.8%)	0.161 (58.1%)
Coarse grain Nb_3Sn	0.100 (17.6%)	0.012 (4.3%)
Number of filaments	*288*	*54*
Twist pitch (mm)	*20*	*12*

[1] From Lasermike diameter measurement.

II.2 Tensile tests: Tensile tests have been performed with a modified tensile test machine "Inspekt table BLUE 05" from Hegwald & Peschke, equipped with an AST KPA-S load cell with a maximum load of 1 kN. Strain is measured with a MTS-clip on extensometer 632.27F-21 with a gauge length of 25 mm.

The moduli of elasticity (E_a) of entire composite wires and extracted filament bundles were determined by recording the engineering stress as a function of strain under decreasing load (see Fig. 3).

Filament bundles have been prepared by etching the Cu matrix only in the wire central part, where the extensometer was attached, leaving the Cu matrix at the wire external parts in order to guarantee an homogeneous load distribution on all filaments. The fialment bundle cross sections that have been used for the E-moduli calculations have been determined by digital image analysis (see Table 1), and confirmed by measurements of the Cu weight loss after etching in nitric acid.

III. Calculated Elastic Properties from Single Crystal Properties

Below the elastic moduli for the polycrystalline Nb_3Sn in the RRP and PIT wires are calculated using Nb_3Sn single crystal elastic constants and the Nb_3Sn grain orientation distribution determined by EBSD. The components $C_{11}=C_{1111}=253.8$ GPa, $C_{12}=C_{1122}=112.4$ GPa, $C_{44}=C_{1212}=39.6$GPa of the stiffness matrix C_{mnpq} of Nb_3Sn single crystal were determined at 300 K in [12]. If $Q_{kl}=\mathbf{e_k}\cdot\mathbf{m_l}$ denotes the rotation matrix between the crystal axes $\mathbf{m}_l$ and the wire axes $\mathbf{e}_k$, ($\mathbf{e}_3$ being the wire direction) the Voigt estimate (upper bound) of the stiffness matrix of a polycrystalline aggregate is the volume average

$$C^V_{ijkl} = \frac{1}{V}\iiint_V Q_{im}\,Q_{jn}\,Q_{kp}\,Q_{lq}\,C_{mnpq}\,dV\,. \qquad (1)$$

Accordingly, denoting by S_{mnpq} the compliance of the single crystal, the Reuss estimate (lower bound) of the stiffness matrix of the polycrystalline aggregate is $C^R_{ijkl} = \left(S^R_{ijkl}\right)^{-1}$ where

$$S^R_{ijkl} = \frac{1}{V}\iiint_V Q_{im}\,Q_{jn}\,Q_{kp}\,Q_{lq}\,S_{mnpq}\,dV\,. \qquad (2)$$

The arithmetic average between these two bounds proposed by Hill [10], i.e. $C^{Hill}_{ijkl} = 1/2\left(C^V_{ijkl} + \left(S^R_{ijkl}\right)^{-1}\right)$, $S^{Hill}_{ijkl} = 1/2\left(\left(C^V_{ijkl}\right)^{-1} + S^R_{ijkl}\right)$ suffers of the inconsistence $C^{Hill}_{ijkl} \neq \left(S^{Hill}_{ijkl}\right)^{-1}$. An averaging procedure that removes this drawback and that has been shown to yield values of the Young's modulus close to the self-consistent estimates as well as measurements for various textures and crystal structures has been suggested in [13]. The elastic components are obtained by applying the iterative procedure

$$\left\{C_{ijkl}^{poly}\right\}_0 = C_{ijkl}^{Hill}, \quad \left\{S_{ijkl}^{poly}\right\}_0 = S_{ijkl}^{Hill}$$
$$\left\{C_{ijkl}^{poly}\right\}_{i+1} = \frac{1}{2}\left(\left\{C_{ijkl}^{poly}\right\}_i + \left\{S_{ijkl}^{poly}\right\}_i^{-1}\right), \quad (3)$$
$$\left\{S_{ijkl}^{poly}\right\}_{i+1} = \frac{1}{2}\left(\left\{S_{ijkl}^{poly}\right\}_i + \left\{C_{ijkl}^{poly}\right\}_i^{-1}\right),$$

until $\left\{C_{ijkl}^{poly}\right\}_i = \left\{S_{ijkl}^{poly}\right\}_i^{-1}$. In the Voigt notation for symmetric tensors, the stiffness matrix of the polycrystalline aggregate with the PIT texture is given below in the wire axes (in GPa)

$$\begin{pmatrix}\sigma_{11}\\ \sigma_{22}\\ \sigma_{33}\\ \sigma_{12}\\ \sigma_{13}\\ \sigma_{23}\end{pmatrix} = \begin{bmatrix} 226.4 & 125.0 & 127.2 & -2.1 & 0.2 & -0.5 \\ 125.0 & 225.5 & 128.1 & -1.5 & -0.7 & -1.2 \\ 127.2 & 128.1 & 223.3 & 3.6 & 0.5 & 1.7 \\ -2.1 & -1.5 & 3.6 & 97.7 & -0.8 & -1.0 \\ 0.2 & -0.7 & 0.5 & -0.8 & 102.2 & 5.5 \\ -0.5 & -1.2 & 1.7 & -1.0 & 5.5 & 104.1 \end{bmatrix} \begin{pmatrix}\varepsilon_{11}\\ \varepsilon_{22}\\ \varepsilon_{33}\\ \varepsilon_{12}\\ \varepsilon_{13}\\ \varepsilon_{23}\end{pmatrix} \quad (4)$$

The wire axes $\mathbf{e}_i$ are identical with the axes in which the EBSD angles were provided (see above). The Young's modulus $E_{\mathbf{e}}$ is the ratio of the axial stress to the axial strain for any uniaxial stress state along a direction $\mathbf{e}$. In the case of a stress applied along one of the axes $\mathbf{e}_i$, $i=1,2,3$, $E_i = E_{\mathbf{e}_i}$ can be immediately obtained by computing the inverse of the corresponding diagonal component of the compliance tensor, i.e. $E_i = 1/S_{iiii}$. In particular, the Young's moduli for the PIT texture in the wire axes are $E_1^{PIT} = 136.0$ GPa, $E_2^{PIT} = 134.3$ GPa and $E_3^{PIT} = 130.2$ GPa and the ratio betwen longitudinal and transversal moduli is $r^{PIT} = E_3^{PIT} / E_{1-2}^{PIT} = 0.96 - 0.97$. For comparison, the Young's modulus of the isotropic aggregate is $E^{iso} = 135.9$ GPa. The properties are roughly transversely isotropic around the wire axis with a Zener anisotropy ratio $A^{PIT} = 2C_{1212}^{PIT} / \left(C_{1111}^{PIT} - C_{1122}^{PIT}\right) = 0.964$. Note that in the case of an exact tranversal isotropy the anisotropy ratio A^{PIT} as defined above is one. Note also that the followed averaging procedure is valid independantly of the symmetry class of the crystal considered (cubic in this work).

For the RRP texture, the estimate of the stiffness in the Voigt notation is

$$\begin{pmatrix}\sigma_{11}\\ \sigma_{22}\\ \sigma_{33}\\ \sigma_{12}\\ \sigma_{13}\\ \sigma_{23}\end{pmatrix} = \begin{bmatrix} 223.2 & 130.6 & 124.8 & 2.9 & 0.3 & 0.9 \\ 130.6 & 222.8 & 125.2 & -0.2 & 0.5 & 0.0 \\ 124.8 & 125.2 & 228.6 & -2.7 & -0.9 & -0.9 \\ 2.9 & -0.2 & -2.7 & 109.5 & 1.3 & 0.8 \\ 0.3 & 0.5 & -0.9 & 1.3 & 97.3 & -3.5 \\ 0.9 & 0.0 & -0.9 & 0.8 & -3.5 & 98.2 \end{bmatrix} \begin{pmatrix}\varepsilon_{11}\\ \varepsilon_{22}\\ \varepsilon_{33}\\ \varepsilon_{12}\\ \varepsilon_{13}\\ \varepsilon_{23}\end{pmatrix} \quad (5)$$

The Young's moduli in the wire axes are: $E_1^{RRP} = 129.8$ GPa, $E_2^{RRP} = 129.2$ GPa and $E_3^{RRP} = 140.0$ GPa. The anisotropy between the longitudinal and transversal directions characterised by $r^{RRP} = E_3^{RRP} / E_{1-2}^{RRP} = 1.08$ and the anisotropy in the transverse plane 1-2 characterised by $A^{RRP} = 2C_{1212}^{RRP} / \left(C_{1111}^{RRP} - C_{1122}^{RRP}\right) = 1.18$ are stronger than for the PIT texture.

The higher Young's modulus in the wire direction for the RRP texture is likely due to the fact that its <001> texture is more intense than in the powder [9]. Indeed, the Young's modulus of the single crystal is maximal in the <001> direction, $E_{<001>}$=184.8 GPa, while $E_{<011>}$=122.1 GPa in the <011> direction. In turn, the <011> orientation dominates in the PIT texture.

The ultrasonic measurements reported in [13] show that the anisotropy ratio $(C_{1111}-C_{1122})/2C_{1212}$ dramatically decreases below room temperature. Hence, no conclusions can be drawn from the preceding results about properties at 4.2 K.

The elastic moduli at 4.2 K have been calculated correspondingly using the components C_{11}=306 GPa, C_{12}=85.7 GPa C_{44}=21.8 GPa of Nb_3Sn single crystal determined at 4.2 K in [12]. Results are summarised in Table 2.

Table 2: Nb_3Sn elastic moduli in axial and transverse directions calculated for the RRP and PIT wires at RT and at 4.2 K.

		PIT B215	RRP #7419
RT	E_{axial}	130	140
	E_{trans}	135	129
4.2 K	E_{axial}	106	127
	E_{trans}	116	104

IV. *Measured E-modulus for the RRP and PIT composite wires and their extracted filaments*

Tensile tests have been performed at room temperature with the entire RRP and PIT composite wires, as well as with the extracted filament bundles. When mounting the clip-on extensometer on the reacted filament bundles, particular care has been taken in order not to damage the brittle filaments. Only measurements with samples where no broken filaments were seen when starting the unloading curve are presented here.

Stress-strain curves for the entire reacted RRP wire and extracted filament bundle are shown in Figure 3. The shape of the filament stress-strain curve is typical for extracted Nb_3Sn filament bundles, and it is probably caused by a re-alignment of the initially bended filaments until the load is uniformly distributed. The E-moduli have been determined from the linear portion of the unloading curves.

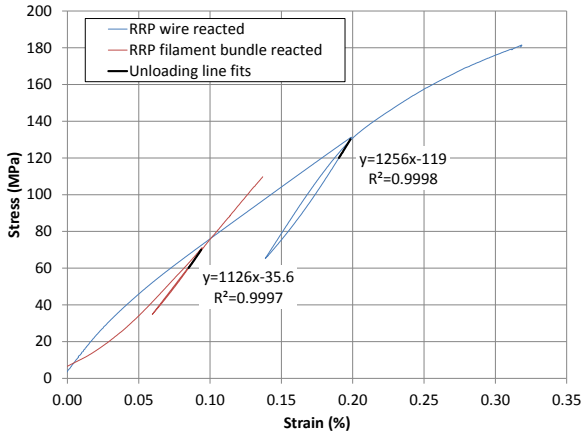

Figure 3: Stress-strain curves measured at room temperature on a reacted RRP wire and its extracted filaments.

In Table 3 the E-moduli of the reacted PIT and RRP wires and their extracted filaments are compared.

Table 3: Comparison of E-moduli in axial direction for the reacted RRP and PIT wires and their extracted filament bundles.

	E-modulus (GPa)	
	PIT B215	RRP #7419
Wire reacted	116±2.3	124±1.7
Filaments reacted	84.8±1.1	114±3.8

V. Discussion and Conclusion

The texturing of the Nb_3Sn filaments causes an elastic anisotropy in PIT and RRP type multifilament wires. In the PIT wire the Nb_3Sn has a preferential <110> orientation and, as a result, the E-modulus at ambient temperature in the axial direction (130 GPa) is smaller than that calculated in perpendicular wire direction (135 GPa). In the RRP wire with a <100> Nb_3Sn texture an E-modulus of 140 GPa in axial direction has been calculated, which is higher than the E-modulus of 129 GPa calculated in the perpendicular direction.

The elastic anisotropy influences the stress in the Nb_3Sn filaments at a certain strain and, thus, can influence the strain limit at which the filaments are permanently degraded. Since a similar Nb_3Sn texture is observed in Ti and Ta-doped RRP wires [9], texturing cannot explain why the irreversible strain limit in Ti doped RRP wires is higher than in Ta-doped RRP wires [19]. In conjunction with the mechanical properties of Nb_3Sn, those of the Nb diffusion barrier may also influence the irreversible strain limit of the composite wire [20,21].

The E-moduli calculations rely on the published Nb_3Sn single crystal elastic constants. A verification of the calculated E-moduli with experimental results is not straight-forward, even at ambient temperature.

The major difficulty in the experimental determination of the Nb_3Sn elastic properties in multifilament wires is that the Nb_3Sn cannot be separated from the unreacted Nb barrier and the filament core. In addition the filaments contain porosity, and it is unclear if the coarse Nb_3Sn grains in PIT filaments, which are probably not well connected, can contribute to the stiffness of the filaments. Consequently, we avoided using the rule of mixture in estimating E-moduli of Nb_3Sn. Nevertheless, the higher E-moduli of the RRP wire and filaments with respect to those of PIT wire and filaments could be explained partly by the higher Nb_3Sn E-modulus in axial direction in the RRP wire. Similar RT Nb_3Sn E-moduli have been published elsewhere [22,23,24].

Fig. 1 from Ref 13 shows that the anisotropy ratio $(C_{1111}-C_{1122})/2C_{1212}$ dramatically decreases from RT to 4.2 K. Hence, no conclusions can be drawn from the RT properties about the 4.2 K properties.

The Young's modulus obtained by averaging the single crystal data from [12] dramatically harden below the phase transformation temperature T_M, while the moduli obtained from ultrasonic data exhibit a smooth profile with almost no hardening below T_M as demonstrated in [25]. This absence of pronounced hardening below T_M was explained in [25] by the ferroelastic behaviour of the tetragonal phase.

The experimental determination of the Nb_3Sn elastic properties at 4.2 K is even more challenging than it is at RT, and therefore it is difficult to verify how reliable the elastic Nb_3Sn single crystal constants are at 4.2 K.

With the tensile set-up used for this study, stress-strain experiments at 4.2 K were not possible. In a previous experiment we found that the non-Cu E-modulus of the PIT B215 wire decreased by about 30% when the wire was cooled from RT to 4.2 K [6]. A significantly lower 4 K E-modulus has been reported for isotropic Nb_3Sn with 1.4 wt.% ZrO_2 precipitates [26].

References

[1] L. Bottura, G. De Rijk, L. Rossi, E. Todesco, "Advanced accelerator magnets for upgrading the LHC", IEEE Trans. Appl. Supercond., vol. 22, 4002008, 2012

[2] L. Thilly P.O. Renault, V. Vidal, F. Lecouturier, S. Van Petegem, U. Stuhr, H. Van Swygenhoven, Appl. Phys. Lett. 88, 91906, 2006

[3] M.T. Naus, P.J. Lee, D.C. Larbalestier, "The interdiffusion of Cu and Sn in internal Sn Nb_3Sn superconductors", IEEE Trans. Appl. Supercond., vol. 10, pp. 983–987, 2000

[4] M. Di Michiel, C. Scheuerlein, "Phase transformations during the reaction heat treatment of powder-in-tube Nb_3Sn superconductors", Supercond. Sci. Technol., vol. 20, L55–58, 2007

[5] M.J.R. Sandim, H.R.Z. Sandim, S. Zaefferer, D. Raabe, S. Awaji, K. Watanabe, "Electron backscatter diffraction study of Nb_3Sn superconducting multifilamentary wire Scr. Mater., vol. 62, pp. 59–62, 2010

[6] C. Scheuerlein, M. Di Michiel, F. Buta, B. Seeber, C. Senatore, R. Flükiger, T. Siegrist, T. Besara, J. Kadar, B. Bordini, A. Ballarino, L. Bottura, "Stress distribution and lattice distortions in Nb_3Sn/Cu multifilament wires under uniaxial tensile loading at 4.2 K", Supercond. Sci. Technol., vol. 27, 025013, 2014

[7] C. Scheuerlein, U. Stuhr, L. Thilly, "In situ neutron diffraction under tensile loading of powder-in-tube Nb_3Sn/Cu composite wires: effect of reaction heat treatment on texture, internal stress state and load transfer Appl. Phys. Lett., vol. 91, 042503, 2007

[8] C. Scheuerlein, M. Di Michiel, F. Buta, "Synchrotron radiation techniques for the characterisation of Nb_3Sn superconductors IEEE Trans. Appl. Supercond., vol. 19, pp. 2653–2656, 2009

[9] C Scheuerlein, G Arnau, P Alknes, N Jimenez, B Bordini, A Ballarino, M Di Michiel, L Thilly, T Besara, T Siegrist "Texture in state of the art Nb_3Sn multifilamentary superconducting wires", Supercond. Sci. Technol., vol. 27, 025013, 2014

[10] R. Hill. The elastic behaviour of a crystalline aggregate. Proc. Phys. Soc., vol. A65, pp. 349-354, 1952

[11] S. Matthies, M. Humbert. On the principle of a geometric mean of even-rank symmetric tensors for textured polycrystals. J. Appl. Cryst., vol. 28, pp. 254-266, 1995

[12] K.R. Keller, J.J. Hanak, "Lattice softening in single crystal Nb_3Sn", Physics Letters, vol. 21, pp. 263 – 264, 1966

[13] W. Rehwald, M. Rayl, R. W. Cohen, G. D. Cody, "Elastic Moduli and Magnetic Susceptibility of Monocrystalline Nb_3Sn", Phys. Rev. B, pp. 363-371, 1972

[14] H. Devantay, J.L. Jorda, M. Decroux, J. Muller, R. Flükiger, "The physical and structural properties of superconducting A15-type Nb-Sn alloys", J. Mater. Sci., vol. 16, pp. 2145, 1981

[15] W. Goldacker, R. Ahrens, M. Nindel, B. Obst, C. Meingast, "HIP synthesized Nb_3Sn bulk materials with extraordinary homogeneity", IEEE Trans. Appl. Supercond., vol. 3, pp. 1322, 1993

[16] J. Zhou, Y. Jo, Z.H. Sung, H. Zhou, P.J. Lee, D.C. Larbalestier, "Evidence that the upper critical field of Nb_3Sn is independent of whether it is cubic or tetragonal", Appl. Phys. Lett., vol. 99, 122507, 2011

[17] M. Cantoni, C. Scheuerlein, P.-Y. Pfirter, F. de Borman, J. Rossen, G. Arnau, L. Oberli and P. Lee, "Sn concentration gradients in Powder-in-Tube superconductors", J. Phys.: Conf. Ser. 234 022005, 2010

[18] C. Scheuerlein, M. Di Michiel, G. Arnau Izquierdo, and F. Buta, "Phase Transformations During the Reaction Heat Treatment of Internal Tin Nb_3Sn Strands With High Sn Content", IEEE Trans. Appl. Supercond., vol. 18(4), 1754, 2008

[19] N. Cheggour, L.F. Goodrich, T.C. Stauffer, J.D. Splett, X.F. Lu, A.K. Ghosh, G. Ambrosio, "Influence of Ti and Ta doping on the irreversible strain limit of ternary Nb_3Sn superconducting wires made by the restacked-rod process", Supercond. Sci. Technol., vol. 23, 052002, 2010

[20] N. Chamdawalla et al., Metall, vol. 40(2), pp. 141-145, 1986
[21] C. Scheuerlein, A. Devred, B. Fedelich, M. Finn, M. Griepentrog, P. El-Kallassi, F. Lecouturier, L. Oberli, B. Rehmer, S. Sgobba, L. Thilly, V. Vidal, "Tensile properties of the individual phases in un-reacted multifilament Nb_3Sn wires", ICMC'06 proceedings, Prague, 2006
[22] M. Hojo, T. Matsuoka, M. Hashimoto, M. Tanaka, M. Sugano, S. Ochiai, K. Miyashita, "Direct measurement of elastic modulus of Nb_3Sn using extracted filaments from superconducting composite wire and resin impregnation method", Physica C 445-448, pp. 814-818, 2006
[23] C.F. Old, J.P. Charlesworth, "The breaking strain of Nb3Sn in a multifilamentary superconductor", Cryogenics, vol. 16, pp. 469-472, 1976
[24] D.S. Easton, D.M. Kroeger, W. Specking, C.C. Koch, "A prediction of the stress state in Nb_3Sn superconducting composites", J. Appl. Phys., vol. 51(5), pp. 2748-2757, 1980
[25] M. Poirier, R. Plamondon, J.D.N. Cheeke, J.F. Bussière, "Elastic constants of polycrystalline Nb_3Sn between 4.2 and 300K", J. Appl. Phys., vol. 55, pp. 3327-3332, 1984
[26] S. L. Bray, J. W. Ekin, R. Sesselmann, "Tensile Measurements of the Modulus of Elasticity of Nb_3Sn at Room Temperature and 4 K", IEEE Trans. Appl. Supercond., vol. 7(2), pp. 1451-1454, 1997